Far Infrared Birefringence versus Other Orientational Measurements of High-Pressure Injection-Molded High-Density Polyethylene

ANTAL BOLDIZAR, *Polymeric Materials,* STELLAN JACOBSSON and SVERKER HÅRD, *Applied Electron Physics, Chalmers University of Technology, S-412 96 Göteborg, Sweden*

Synopsis

Far infrared (FIR) birefringence is a new tool for measuring orientation in semicrystalline polymers. In this work FIR birefringence of high-pressure injection-molded high-density polyethylene (HDPE) was compared with wide-angle X-ray scattering (WAXS) and shrinkage for the first time. An indirect measure of orientation was obtained by differential thermal analysis (DTA). The content of high-temperature melting crystals was found to increase with increasing orientation. A high correlation was found between FIR birefringence and the other orientational measurements. Contrary to the other orientational methods used, FIR birefringence does not saturate with highly oriented samples. It is furthermore faster, nondestructive, and can be used for probing fairly thick samples.

INTRODUCTION

Far infrared (FIR) wavelengths, ~ 100 μm, have been used successfully to measure the birefringence of injection-molded high-density polyethylene (HDPE).[1,2] A major advantage of the method is that crystalline polymer samples thick enough to be opaque at visible wavelenths can be measured. So far the FIR birefringence has only been compared with the modulus of the samples.[2] In this work we quantitatively compare the FIR birefringence with conventional orientational measurements for the first time. These were obtained by X-ray diffraction and by shrinkage following heating of the samples. A third orientational measurement, although indirect, was obtained through differential thermal analysis (DTA). Here the crystallinity that is caused by the high-temperature melting crystals only was determined. Such crystals have been shown to form and orient themselves in the flow direction under shearing conditions typical of injection molding.[3] To allow these measurements, the samples had to be sliced at a thickness of ~ 100 μm. This demanded that the accuracy of the existing FIR method had to be improved prior to the measurements.

There is no simple method to interpret FIR birefringence directly. This is because it is determined by the detailed orientation, composition, structure, and FIR properties of the probed polymer molecules, parameters which are

Journal of Applied Polymer Science, Vol. 36, 1567–1581 (1988)
 CCC 0021-8995/88/071567-15$04.00

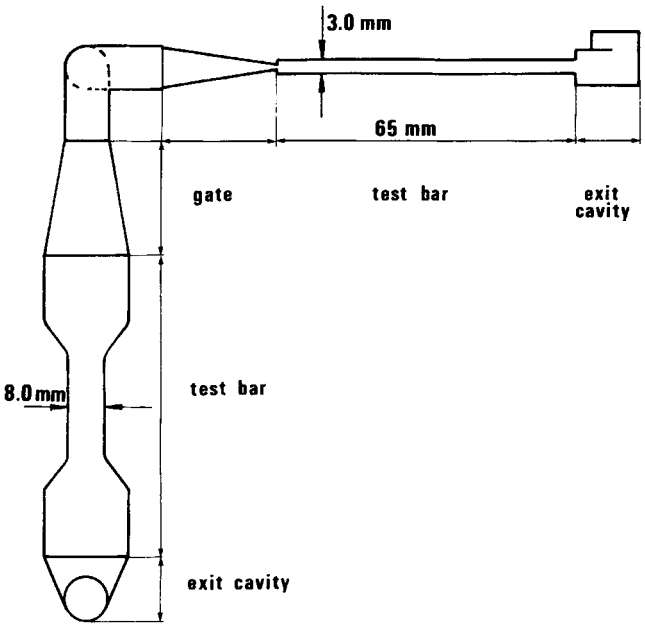

Fig. 1. Shape of the moldings.

generally unknown.* FIR birefringence shares this characteristic with other orientational measurements and since the different techniques weigh these parameters differently, no two orientational measurements are equivalent. FIR birefringence should be regarded as a method that gives partly new, complementary information about polymer orientation rather than one which competes with conventional methods.

MATERIALS AND SAMPLE PREPARATION

The material used for investigation was extrusion-grade HDPE (DMDS 2215, Unifos, Sweden). This somewhat unusual material was chosen because it yields high stiffness and strength to the moldings when injection molded using a specific high-pressure process described elsewhere.[4] Using this process, our test bars were manufactured at molding pressure, 300 MPa, melt temperature, 190°C, and mold temperature, 30°C. Flow rates were 7, 12, 17, and 23 cm^3/s. It was found previously[5] that the stiffness of the test bars shows a pronounced maximum when manufactured at the stated pressure and temperature and at a flow rate of 17 cm^3/s. The shape of the moldings is shown in Figure 1.

The test bars used in the FIR birefringence, WAXS, and DTA measurements had a thickness of 3.0 mm, which allowed us to produce good quality, plane-parallel microtome slices. Such slices are required if reliable FIR bire-

*Note that the interaction of FIR radiation with real matter is so complex that even for the simplest materials, namely single crystals, the index ellipsoid (birefringence) cannot be calculated theoretically. Instead one has to rely on measurements.

fringence data are to be obtained. The microtoming procedure consisted of first planing off the sides of the original dog-bone test bar to give it a rectangular shape, having a width of 8 mm, its length being unchanged. The test bar was next clamped at its sides in the microtome apparatus (Leitz 1400 base sledge microtome). Microtoming was performed with a 5 mm wide knife blade along the full length of the test bar. With this procedure the test bar still remained straight after about twenty 100 μm slices had been cut. Attempts to use a microtome blade that was wider than the test bar width were unsuccessful because of problems in obtaining a good enough adhesive joint between the test bar polyethylene surface and its support.

The quality of a microtome slice could be judged by comparing the thickness as measured with a micrometer and as measured with the FIR interferometer. When determining the sample thickness using the FIR interferometer, the index of refraction was taken to be 1.52. The thickness was measured with the electric field directed in the flow direction. We observed that reproducible birefringence values were obtained when the two thicknesses differed by less than 10 μm. (Another quality measure of the microtomed slices is given by the modulation depth of the FIR interferograms, which we found was different for different samples.) The measured slice thicknesses were typically $\sim$ 120 μm, compared with the microtome setting of 100 μm. This discrepancy could be due to sample contraction caused by the microtoming.

METHODS OF MEASUREMENTS

FIR Birefringence of Thin Samples

A main aim of this work was to compare the FIR birefringence Δn with other orientational methods of measurement: wide angle X-ray scattering (WAXS) and differential thermal analysis (DTA). It is desirable to apply all three methods to the same samples. Initially this could not be done satisfactorily because at sample thicknesses of about 100 μm, which the latter two methods demand, the accuracy of the Δn measurement was too poor. After completing the birefringence versus shrinkage measurements (last section of this paper), we succeeded in meeting this demand by modifying the FIR interferometer, thus increasing its accuracy an order of magnitude. The interferometer previously described in Refs. 1,2 was modified in the following ways: The sample mounted on a precision rotator was rotated during measurement at fixed, linear FIR beam polarization. Care was taken to align the focused FIR beam at the center of rotation of the sample. By focusing, the FIR laser beam was only $\sim$ 1 mm wide, which is five times smaller than the width of the sample, making truncation effects of the laser beam insignificant. (A too-wide beam will affect the phase determination adversely.) Another improvement is that the time of recording and evaluating an interferogram was reduced from 4 min to 30 s, which makes ambient temperature drift correspondingly less disturbing. A simplified drawing of the FIR interferometer for thin samples is shown in Figure 2. The wavelength used was 70.5 μm.

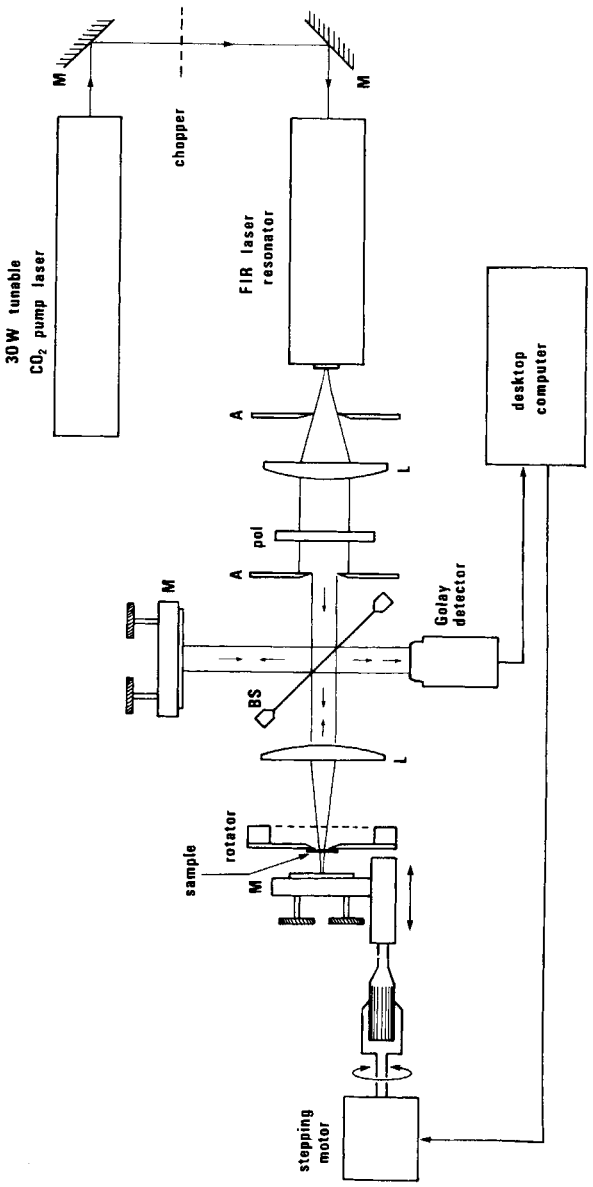

Fig. 2. FIR laser interferometer used in measurements of thin samples. M = mirror, A = aperture, L = lens, pol = polarizer, BS = beam splitter.

Wide-Angle X-ray Scattering (WAXS)

The microtomed slices were measured using a commerical precession WAXS apparatus (Nonius, Delft, The Netherlands), the radiation being incident normal to the section surfaces of the samples, employing the CuK_α line (1.5418 Å). Temperature was 6°C. The distance between sample and the planarly mounted film was 10.00 cm, the exposure time being ~ 1 h. The geometry allowed several full diffraction rings at scattering angles $\theta \lesssim 32.0°$ to be recorded. The majority of the diffraction rings could be satisfactorily interpreted as being due to an orthorhombic crystal lattice with axes 7.40, 4.94, and 2.55 Å.[6] We chose to evaluate only the diffraction ring at $\theta = 27.6°$, since this ring was reasonably strong and yet revealed no significant film saturation contrary to other rings. The chosen diffraction ring is presumably

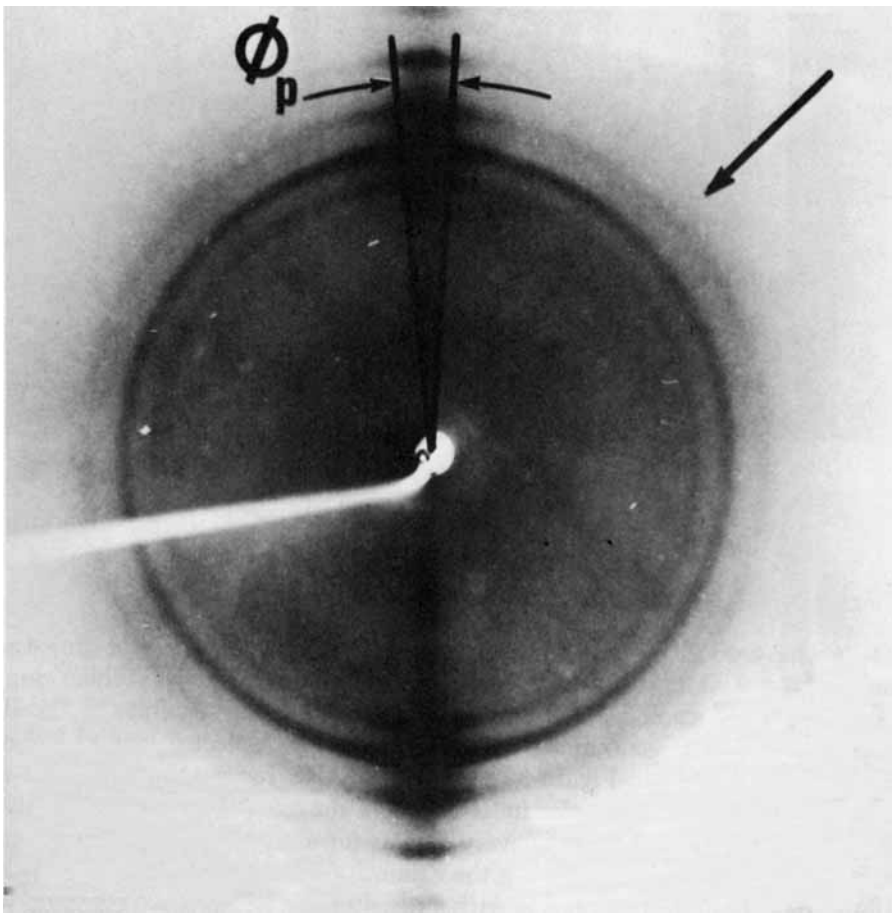

(a)

Fig. 3. WAXS recording exemplifying (a) high and (b) low orientation respectively. The arrows show the evaluated ring. (a) Sample taken from high shear region, halfway between surface and center of the test bar. $\phi_p \simeq 11°$. (b) Sample taken from low shear, core region of the test bar. $\phi_p \simeq 67°$.

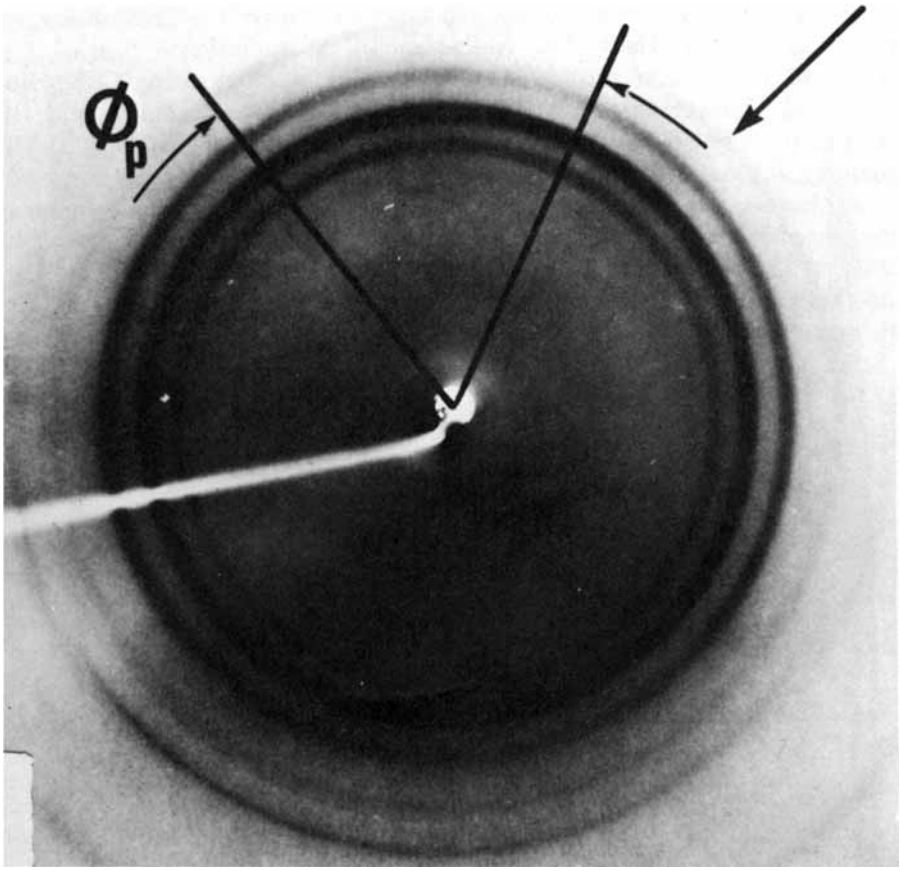

(b)

Fig. 3. (*Continued from the previous page.*)

not to be associated with the orthorhombic crystal lattice, but processed polyethylene is known to exhibit several additional reflections.[7] Which ring is chosen for evaluation is of little importance since all rings exhibit very similar angular intensity distributions, which, by definition, reflect the sate of orientation of the samples. Figure 3 shows two WAXS recordings, which clearly demonstrate that the samples indeed were of different degrees of orientation and that the recorded rings are very similar for a given sample. The orientation was quantified by measuring the azimuthal film attenuation distribution along the chosen diffraction ring with a densitometer. After subtraction of the amorphous attenuation background distribution, measured next to the ring, the full width at half maximum of the attenuation peak ϕ_p (expressed in azimuthal angle) was determined. The quantity ϕ_p or its inverse is a convenient measure of orientation.[8]

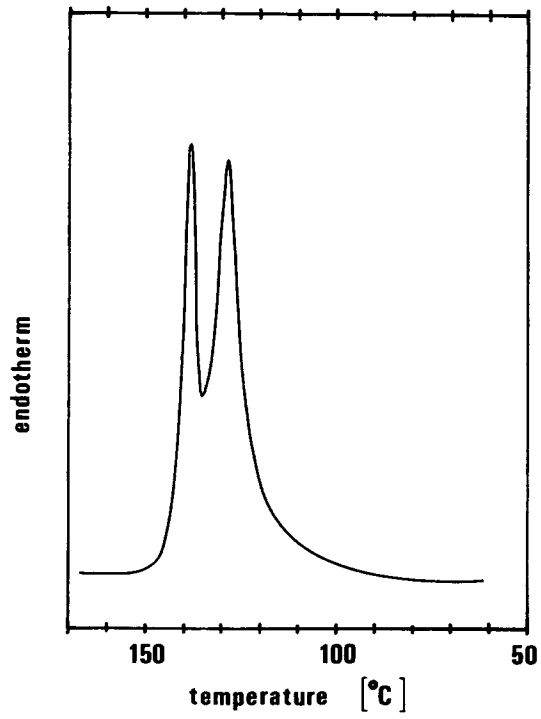

(a)

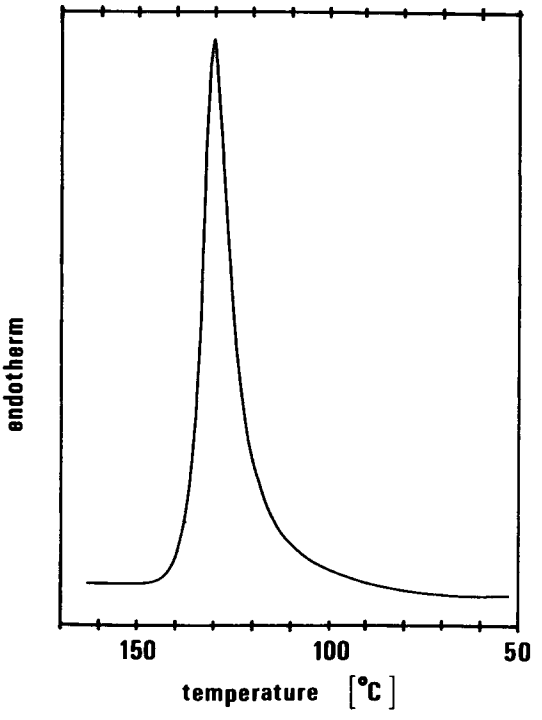

(b)

Fig. 4. DTA recordings of (a) sample from high-shear region, high-temperature melting crystallinity $c \simeq 27\%$ and (b) low-shear, core region, $c \simeq 0\%$. Samples are the same as shown in Fig. 3.

Differential Thermal Analysis (DTA)

A Mettler TC 2000 apparatus was used for the DTA measurements. Sample thickness and mass were ~ 100 μm and ~ 1 mg, respectively. The samples were contained in standard aluminum crucibles. The reference was an empty, identical crucible. Heating rate was 10°C/min. The experiment was conducted in air at atmospheric pressure. Heat of fusion used for crystallinity evaluation was 293 J/g.[9] Two distinct, yet not completely separated melting peaks were observed at 129° and 138°C. These melting points were found to vary less than ± 2°C.[5] The relative strengths of the two peaks varied with the distance from the surface d which is demonstrated in Figure 4. The peak centered around 129°C is due to crystals that form under ordinary conditions in PE, whereas the peak at 138°C should be due to shear-induced crystals[3] (cf. Fig. 4). Because of incomplete separation of the two measured peaks, there is neccessarily some uncertainty involved when determining the content of either crystal type, the relative uncertainty of the DTA values estimated to be less than $\pm 10\%$.

RESULTS AND DISCUSSION

Data are obtained for the microtomed samples, measured at their midpoints which are located 33 mm from the gates. Part of the cross-section of the test

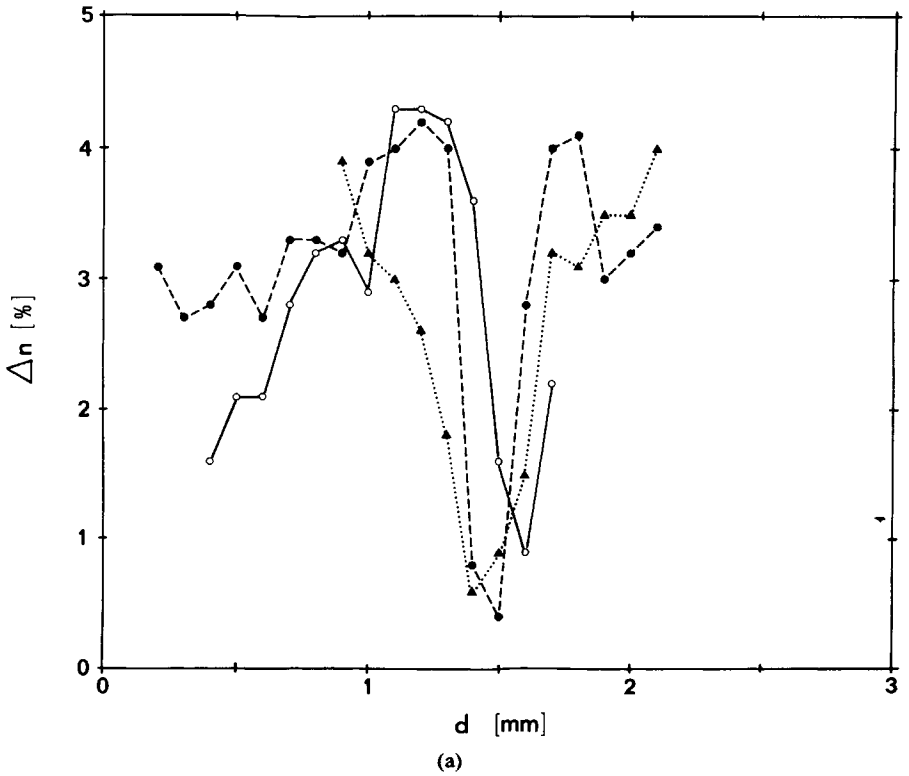

(a)

Fig. 5(a). Measured FIR birefringence Δn versus depth from surface d at the midpoint of HDPE test bars #I(●), #II(○), and #III(▲), injection molded at 300 MPa and at flow rates 12, 17, and 23 cm^3/s, respectively. Wavelength: 70.5 μm. Full test bar thickness: 3.0 mm.

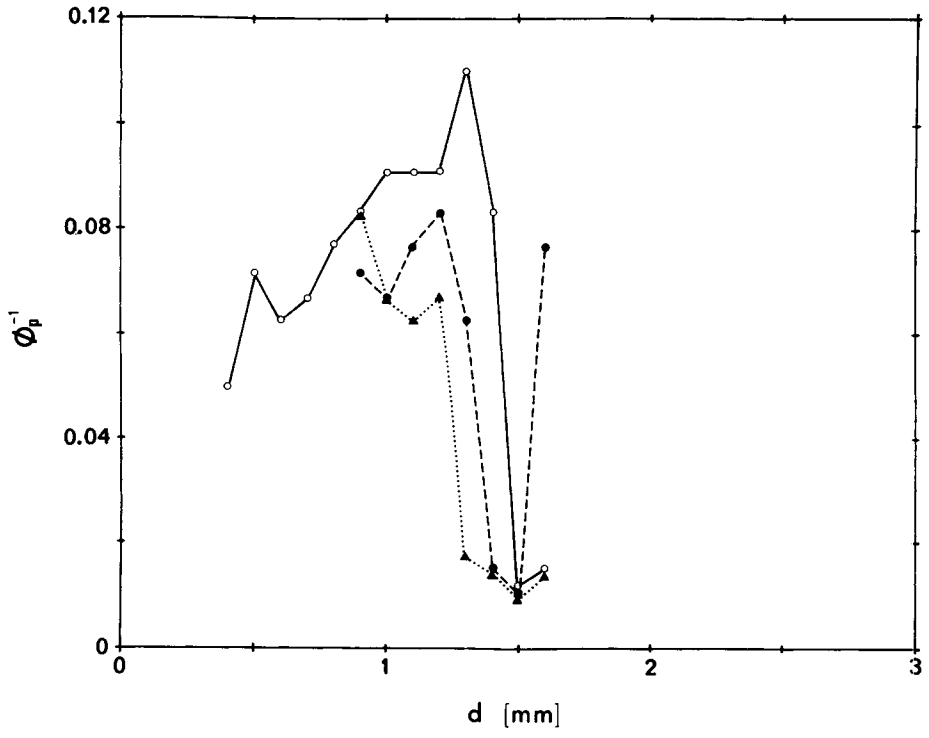

(b)

Fig. 5(b). WAXS orientational measure ϕ_p^{-1} versus depth from surface d at midpoint of the HDPE test bars #I, #II, and #III of Fig. 5a. ϕ_p = Full width at half maximum of diffracted intensity peak (cf. Fig. 3). Full test bar thickness: 3.0 mm.

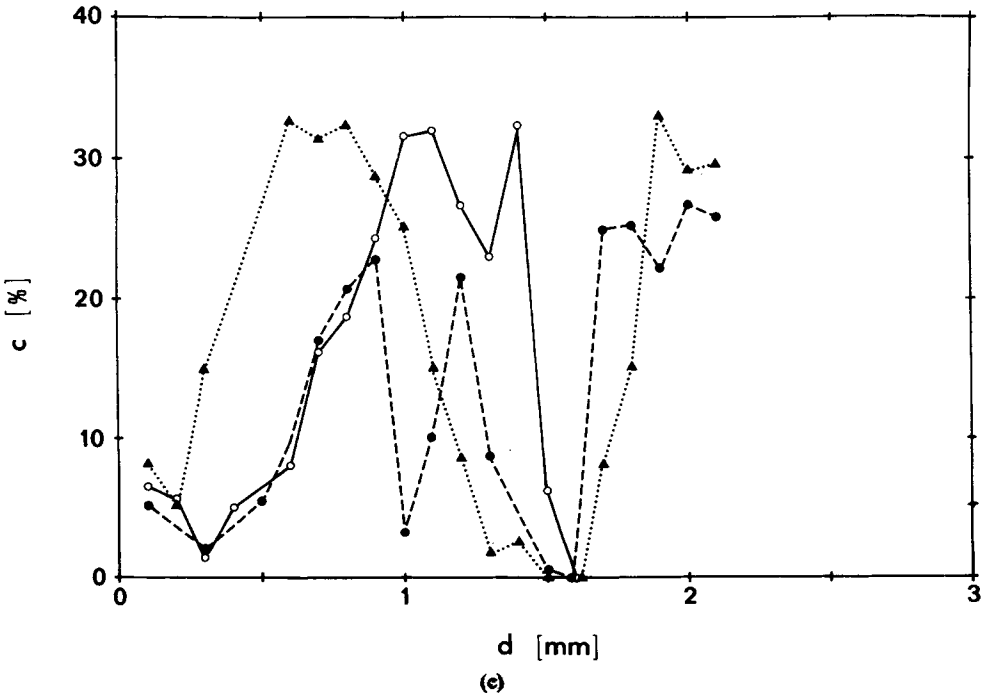

(c)

Fig. 5(c). High-temperature melting crystallinity c obtained by DTA, versus depth from surface d at midpoint of the HDPE test bars #I, #II, and #III of Fig. 5(a). Full test bar thickness: 3.0 mm.

bars was mapped by all three methods. From Figure 5 it can be seen that the two direct orientational mesurements Δn and ϕ_p^{-1} as well as the indirect (crystallinity) measurement c show the same general features, for all three test bars: The core region is oriented the least and there appears to be an orientation maximum at a depth of ~ 1.2 mm. The observed orientation maximum is most likely situated within the region of high shear during injection and was expected (see Ref. 10). Likewise, one should expect a lower orientation in the low shear core region.[10] Note in Figure 5 that test bar #II, which has the highest stiffness, clearly is the most oriented one [Figs. 5(a) and 5(b).]. It also has the highest content of high temperature melting crystals [Fig 5(c)]. Furthermore, Figure 5 shows that at a given depth the three test bars generally follow the same sequential order in Δn, ϕ_p^{-1}, and c. This indicates measuring accuracy is good.

FIR measurements not shown in Figure 5 were further made at two or three other locations along the microtome slices. It was found that test bar #I varied much more than did test bars #II and #III. The birefringence of the latter test bars was almost constant along many slices. Visually the slices microtomed from test bar #I, which was molded at the lowest flow rate, showed varying transparency contrary to those from test bars #II and #III, the sizes of the inhomogeneities being roughly the same as the width of the FIR laser beam. This might be an indication of insufficient injection flow rate for test bar #I.

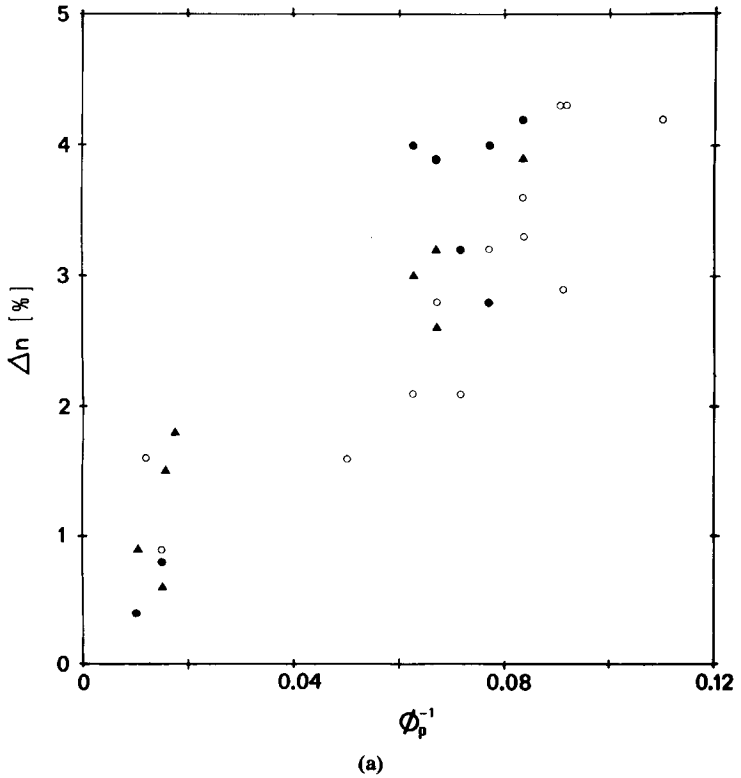

(a)

Fig. 6(a). FIR birefringence Δn versus WAXS orientational measure ϕ_p^{-1}. Data complied from Fig. 5 using the same symbols.

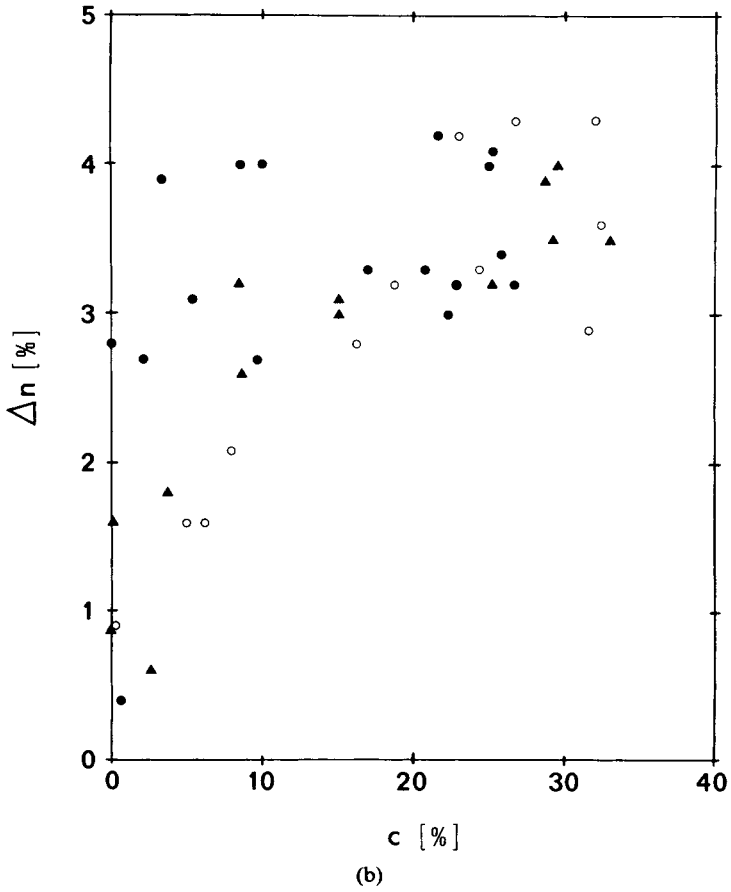

(b)

Fig. 6(b). FIR birefringence Δn versus high-temperature melting crystallinity c. Data complied from Fig. 5 using the same symbols.

The possible existence of systematic error when performing birefingence measurements of microtomed slices can be investigated by comparing the average birefringence taken over all the measured slices for one test bar with the birefringence of a nonmicrotomed test bar manufactured under similar conditions. Since the average values 3.2, 2.8, and 2.5% which we obtained for test bars #I, #II, and #III, respectively, compare quite well with previous measurements of nonmicrotomed test bars[1,2] systematic Δn errors are likely to be small.

The two direct orientational measurements Δn and ϕ^{-1} seem to correlate fairly well, according to Figure 6(a). Note that ϕ_p^{-1} specifically measures orientation of crystals, whereas Δn also includes a contribution from the amorphous parts of the sample. This fundamental difference between the two measurements should explain part of the data scatter in Figure 6(a).* Other

*On visual inspection of the WAXS photos, we find that for some samples a high crystal orientation (ϕ_p^{-1} high) is not accompanied by a high amorphous orientation. Indeed for these particular samples the Δn values are only moderately high.

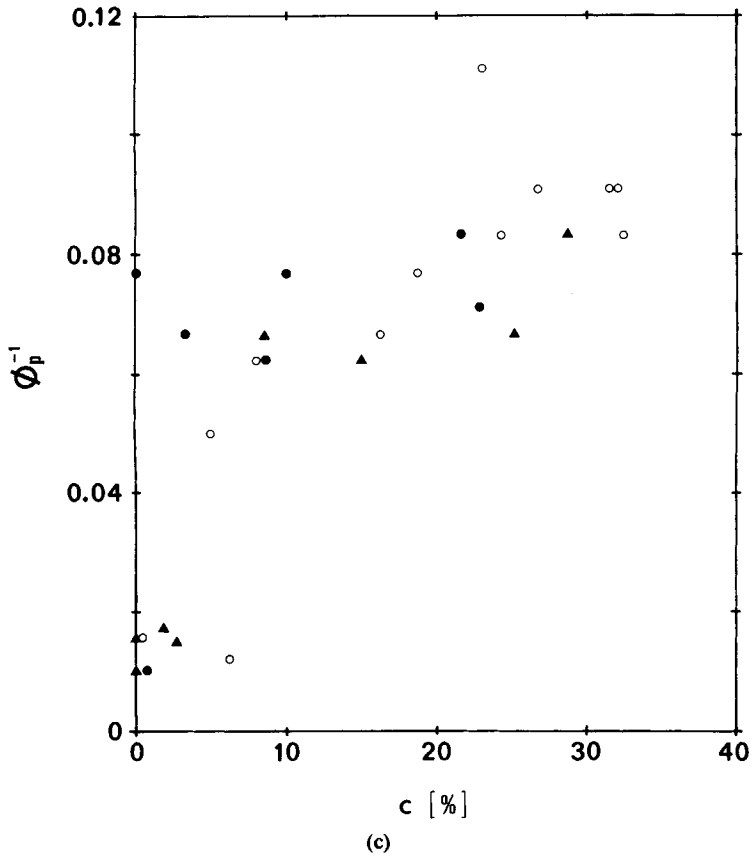

Fig. 6(c). WAXS orientational measure ϕ_p^{-1} versus high-temperature melting crystallinity c. Data compiled from Fig. 5 using the same symbols.

contributing factors are the relative uncertainty in ϕ_p^{-1}, $\pm 15\%$, and the absolute Δn uncertainty 0.0008.

From Figure 6(b) it is clear that Δn and c do not correlate as strongly as Δn and ϕ_p^{-1}. However, there seems to be a definite lower boundary to the data points in Figure 6(b) indicating, in agreement with Keller and Odell,[3] that the high-temperature melting crystals indeed are present only when orientation is significant. Although not quite so clear, the same behavior can be seen in Figure 6(c), which relates ϕ_p^{-1} and c. A final observation to be made in Figure 6(b) is that Δn never exceeds 4.3% irregardless of c.

FIR Birefringence versus Shrinkage Measurements

The measurements reported in this section FIR birefringence Δn versus shrinkage S, were actually conducted before those reported in the preceding sections and with a lower Δn measurement accuracy. Therefore a 1 mm test bar thickness was chosen, which is large enough to allow accurate Δn measurements yet small enough for reasonably accurate shrinkage measurements to be made (Fig. 7). Apart from the thickness, the test bars had the same

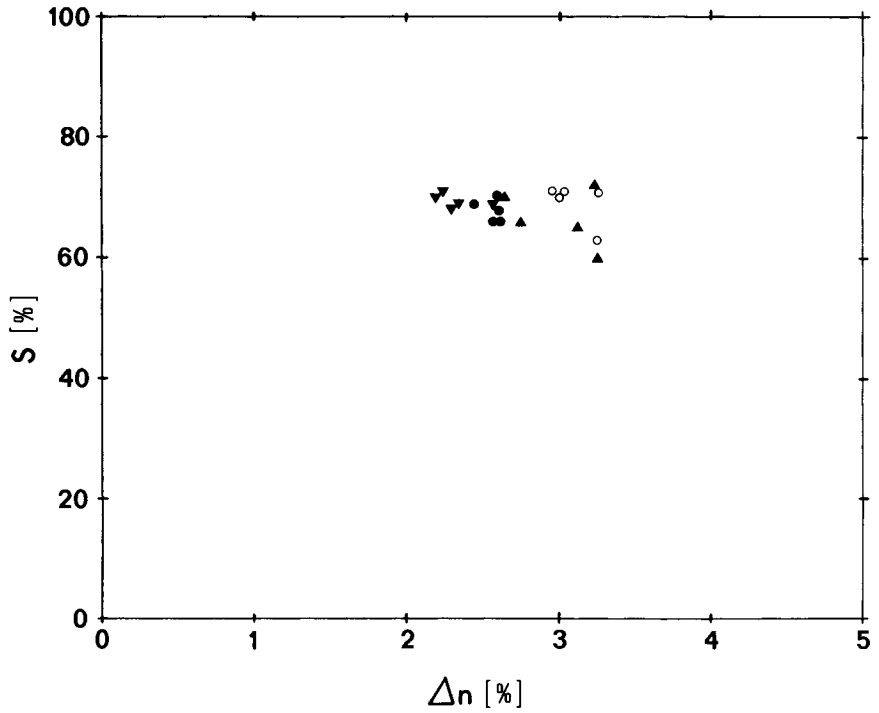

Fig. 7. Shrinkage versus FIR birefringence for 1 mm thick HDPE test bars manufactured at flow rates: 7(▼) 12(●), 17(○), and 23(▲) cm^3/s. Molding pressure was 300 MPa.

dimensions as shown in Figure 1. We estimate the FIR interferometer phase determination inaccuracy could at times have been as high as ± 5 degrees, which corresponds to a Δn inaccuracy of $\pm 3\%$ for the 1 mm thick samples. The width of the FIR beam was 5 mm and the wavelength was 118.8 μm.

The shrinkage measurements of the 1 mm thick samples were performed at 141°C during 10 min in silicon oil. This particular choice of temperature and duration of the shrinkage procedure had previously been found to be adequate for these samples. The dimensions of the samples prior to measurement were $5 \times 10 \times 1$ mm. The presented shrinkage are corrected for volume change. The spread of data for samples manufactured under identical conditions when measured at the same location on the test bars is $\pm 5\%$.* Each sample was measured with both FIR birefringence and shrinkage methods at the midpoint of the test bar. The result is presented in Figure 7. Note that the Δn-values span a considerable range. This is because the samples were molded at four different mass flow rates, which affects the orientation (and the modulus) considerably. The high degree of orientation gives rise to high shrinkage values. Contrary to Δn, the shrinkage values seem to be saturated,

*Due to the layered structure of the injection-molded test bars the shrinkage does not occur uniformly, which results in more or less deformed shrunk samples. This makes the shrinkage measurements for thick samples less accurate than for thin ones. In Figure 7, the most deformed samples were excluded. When calculating shrinkage for a particular sample we used its *average* length and width changes.[11]

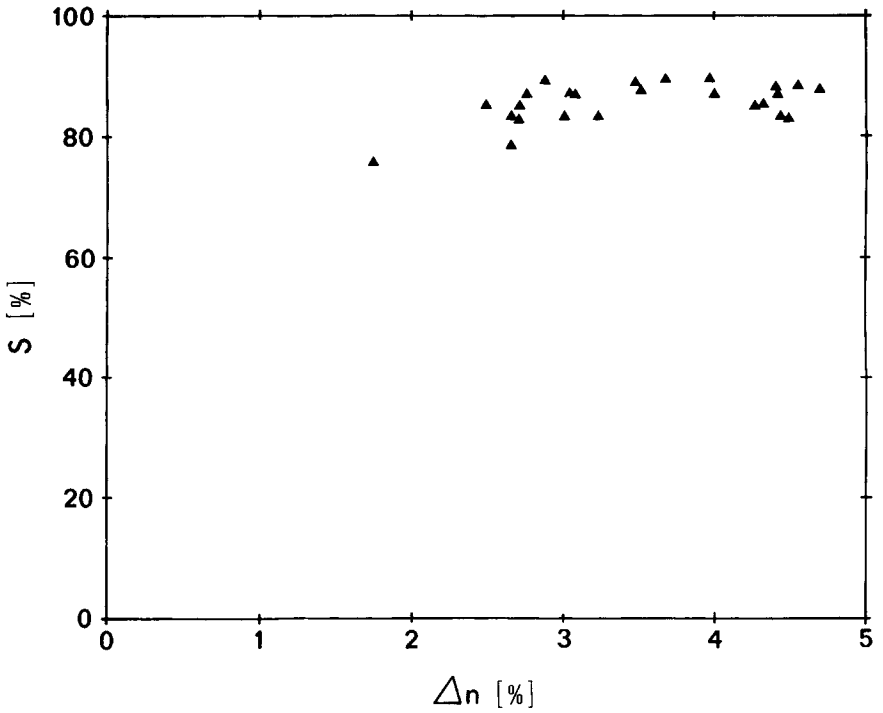

Fig. 8. Shrinkage versus FIR birefringence for 100 μm sliced samples of two 1 mm thick HDPE test bars manufactured at 23 cm^3/s flow rate. Molding pressure was 300 MPa.

however (see Fig. 7). Figure 7 further shows that the highest Δn values are obtained at a flow rate of 17 cm^3/s, which also was found to produce test bars with the highest modulus, ~ 11 GPa.[5]

Although, the phase-determination accuracy was not quite satisfactory, we also performed birefringence versus shrinkage measurements of sliced samples, the results of which are shown in Figure 8. Because of the somewhat limited accuracy, these measurements should be regarded with a certain degree of caution. We chose to report them since comparing with Figure 7 they seem quite reasonable. This is because: (a) Δn values range is larger than in Figure 7, due to the layered structure of the test bars. (b) Shrinkage values are higher on the average than in Figure 7. (c) Average data follow a trend toward the origin of the coordinate system.

SUMMARY

Generally, these measurements show that FIR birefringence correlates well with X-ray, shrinkage, and crystallinity orientational measurements. However, as might be expected, there is not a one-to-one correspondence between the different measurements. Contrary to the X-ray and shrinkage measurements, the FIR birefringence does not seem to saturate at high orientations. Furthermore, it is faster, nondestructive, and likely to be more accurate. It would now be desirable to further assess the potentials and limitations of the new FIR birefringence technique, by conducting other measurements of well characterized polymer samples.

The authors wish to thank Professor Mikael Rigdahl for helpful discussions and a reviewer for valuable suggestions. The WAXS recordings were made at the Department of Inorganic Chemistry, Chalmers University of Technology. This work was supported by two grants from the Swedish Board for Technical Development.

References

1. S. Jacobsson and S. Hård, *Rev. Sci. Instrum.*, **53**, 1012 (1982).
2. S. Jacobsson, S. Hård, and A. Boldizar, *J. Polym. Sci.*, **22**, 471 (1984).
3. A. Keller and J. A. Odell, *J. Polym. Sci., Polym. Symp.* **63**, 155 (1978).
4. J. A. Månson and M. Rigdahl, *Plast. Rubb. Proc. Appl.*, **3**, 229 (1983).
5. A. Boldizar, J. Kubát, and M. Rigdahl, *J. Appl. Polym. Sci.*, submitted.
6. P. R. Swan, *J. Polym. Sci.*, **56**, 403 (1962).
7. P. H. Geil, *Polymer Single Crystals*, Interscience, New York, 1963, p. 51.
8. S. L. Aggarwal, G. P. Tilley, and O. J. Sweeting, *J. Polym. Sci.*, **51**, 551 (1961).
9. A. P. Gray, *Thermochimica Acta* **1**, 563 (1970).
10. Z. Tadmor, *J. Appl. Polym. Sci.*, **18**, 1753 (1974).
11. G. Menges and G. Wübken, *Plastverarbeiter*, **23**, 318 (1972).

Received July 10, 1986
Accepted February 22, 1988